

## Supplementary Figure Legends

### **Supplementary Figure S1: Phenolic inhibitors hindered anaerobic xylose consumption.**

*E. coli* RL3000 was grown in M9 minimal medium, 0.25% (w/v) xylose until the culture reached an early exponential phase ( $OD_{600} \sim 0.2-0.3$ ) before it was exposed to 2.75 mM or 5.5 mM feruloyl amide, coumaroyl amide, or ferulic acid. Concentrations of xylose remained in the culture over time were quantified using LC-MS. Growth rates (/hour) and xylose uptake rates (mM/hour/ $OD$ ) were obtained from nonlinear least-squares (curve-fitting). The extrapolated rates were normalized to those of the controls. Bars represent means of two biological replicates  $\pm$  SEM.

### **Supplementary Figure S2: Feruloyl amide and coumaroyl amide are major contributors to anaerobic growth inhibition of *E. coli*.**

**(A)** Cells were grown in an absence of phenolic inhibitors until early exponential phase ( $OD_{600} \sim 0.2$ ) The cultures were then treated with either of lignin-derived phenolic inhibitor (LDPI) cocktail or feruloyl amide combined with coumaroyl amide. 1X concentrations of LDPI cocktail (see also Figure 1 and Table S1) led to strong anaerobic growth inhibition. 0.5X concentration (2.75 mM) of feruloyl amide and coumaroyl amide (each) was sufficient to account for the same degree of inhibition observed in LDPI cocktail treatment.

**(B)** Inhibitory effects of LDPIs are pronounced in cells grown in xylose. Anaerobic exponential cultures ( $OD_{600} \sim 0.2-0.3$ ) in LDPI-free media with either xylose or glucose were introduced to 1.375 mM, 2.75 mM, or 5.5 mM of feruloyl amide, coumaroyl amide, or ferulic acid.

### **Supplementary Figure S3: Anaerobic growth inhibition by ferulic acid.**

#### **(A) Ferulic acid treatment leads to different alterations in intracellular metabolite levels compared to those in feruloyl amide and coumaroyl amide-treated cells.**

Exponential *E. coli* cultures grown anaerobically on xylose were treated with 5.5 mM ferulic acid. Intracellular metabolites were extracted at 10, 30, 60, 120, 180, and 240 min after exposure to ferulic acid and measured by LC-MS. Metabolite levels of treated samples were normalized against those of controls at each corresponding time points. Metabolites whose level increases upon phenolic amide treatment are shown in shades of yellow and those that decreases are shown in shades of blue. The data represents the averages of two biological replicates.

**(B) Ferulic acid leads to anaerobic growth inhibition of *E. coli*.** Anaerobic *E. coli* was grown in an absence of inhibitor before it was introduced to 5.5 mM ferulic acid at early exponential growth (arrow).

**(C) PRPP accumulation in the presence of ferulic acid.** While PRPP sharply accumulates (at 10 min after treatment) in the presence of feruloyl amide and coumaroyl amide (Figures 1C, 3), the accumulation is not drastic in the presence of ferulic acid. Bars represent means of four biological replicates  $\pm$  SEM.

**(D) Impeded biosynthesis of deoxynucleotide in the presence of ferulic acid.** Anaerobic, exponential culture of *E. coli* was exposed to 5.5 mM ferulic acid for 5 min before switched into a medium containing  $^{13}\text{C}$ -xylose.  $^{13}\text{C}$  incorporation was allowed for 0, 0.5, 1, 2, 4, 7, 10, and 15 min before quenching. While synthesis of ribose-5-phosphate (ribose-5-P), glutamate, and ATP was comparable between the control and ferulic acid-treated samples, biosynthesis of dCTP was impeded in the presence of ferulic acid.

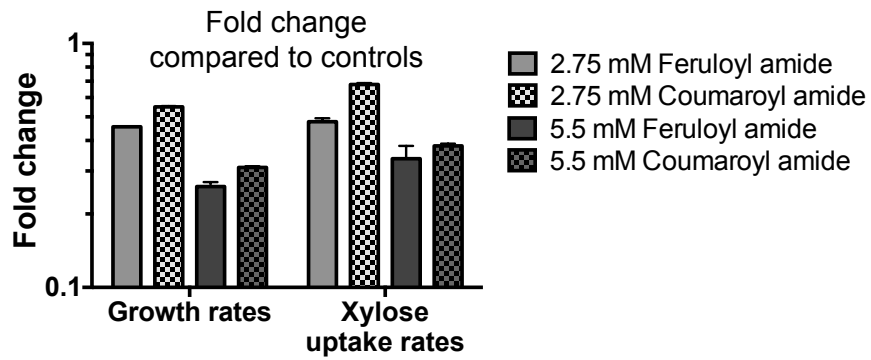
**Supplementary Figure S4: Feruloyl amide inhibits nucleotide biosynthesis at both 5 minutes (short-term) and 2 hours (long-term).** Anaerobic *E. coli* culture in minimal medium with non-labeled xylose was exposed to 5.5 mM feruloyl amide for either 5 minutes (short-term) or 2 hours (long-term) before it was switched to 1, 2  $^{13}\text{C}$ -xylose-containing medium. Samples for intracellular metabolite analysis were taken at 0.5, 1, 2, 4, 7, 10, and 15 min thereafter. The blue-to-red gradient represents the amount of  $^{13}\text{C}$ -label incorporation (sum of all  $^{13}\text{C}$ -labeled forms) into each metabolite as a fraction of its total pool; for each metabolite, the lowest value (non-labeled) was set to blue while the highest  $^{13}\text{C}$ -label fraction value in control samples was set to red. The data represent the average of two biological replicates.

**Supplementary Figure S5: Complete inhibition of nucleotide *de novo* biosynthesis in the presence of phenolic amide inhibitors.** Fragmentation (LC-MS/MS) analysis from the  $^{13}\text{C}$  isotopic tracer experiments described in Fig. 2 showed no  $^{13}\text{C}$  incorporation into nucleobases (adenine of ATP and uracil of UTP) in the presence of feruloyl amide while  $^{13}\text{C}$ -carbon was incorporated into both phospho-ribose sugar and nucleobases in the control. The same pattern was observed in coumaroyl amide-treated cells. The data represent identical results from two biological replicates.

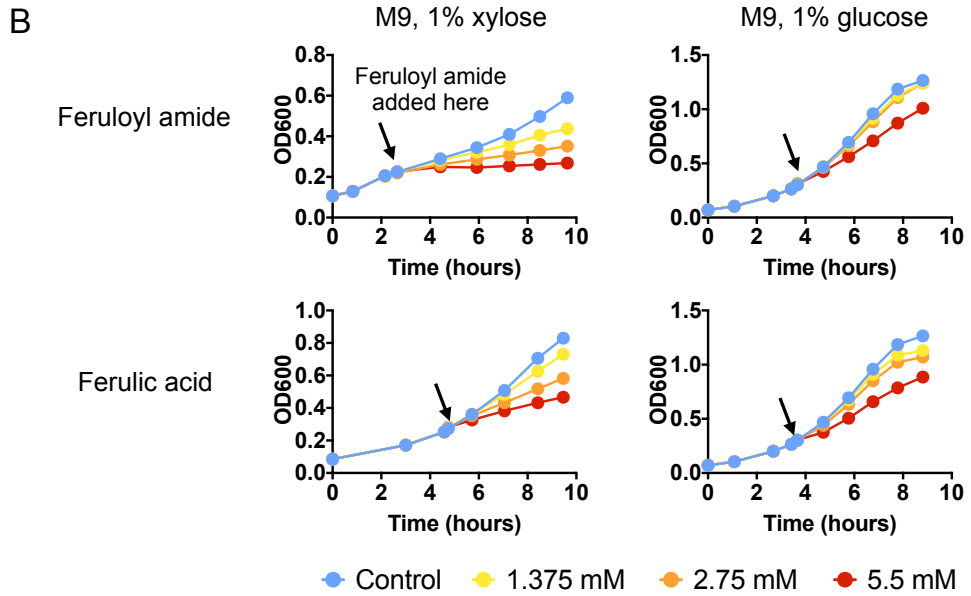
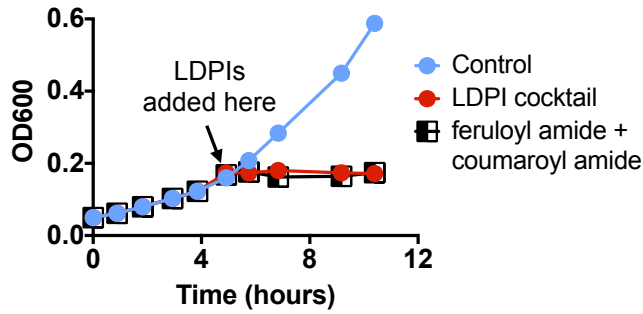
**Supplementary Figure S6: Nucleoside supplementation rescued growth inhibition by phenolic inhibitors. (Top) Feruloyl amide. (Middle) Coumaroyl amide. (Bottom) Ferulic acid.** *E. coli* was grown anaerobically with xylose and supplemented with 0, 0.25, or 0.75 mM of nucleosides (adenosine, guanosine, cytidine, thymidine, and uridine). Exponential culture ( $\text{OD}_{600}$  0.2-0.3) was then divided into individual flasks containing 2.75 mM feruloyl amide, coumaroyl

amide, or ferulic acid. Cell growth was measured using OD<sub>600</sub>. This graph is a representation of 2 independent experiments that gave identical results.

Xylose uptake rates (mM/hour/OD)		
	2.75 mM treatment	5.5 mM treatment
Control	4.593 ± 0.171	
Feruloyl amide	2.196 ± 0.152	1.548 ± 0.248
Coumaroyl amide	3.119 ± 0.116	1.747 ± 0.110



A Feruloyl amide and coumaroyl amide account for inhibitory effects of LDPI cocktail



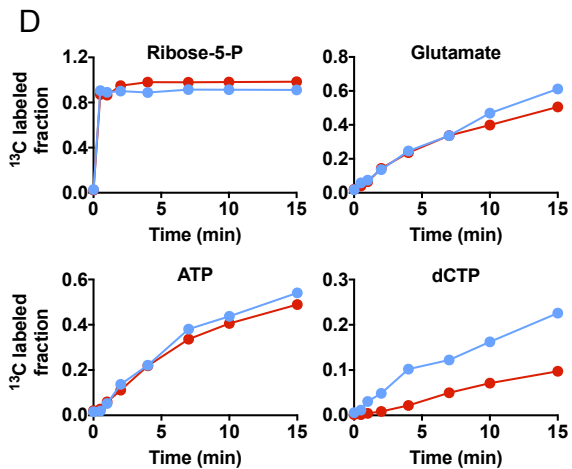
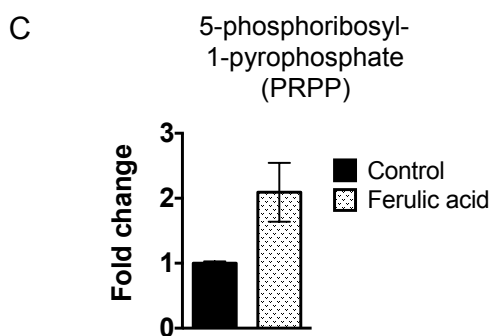
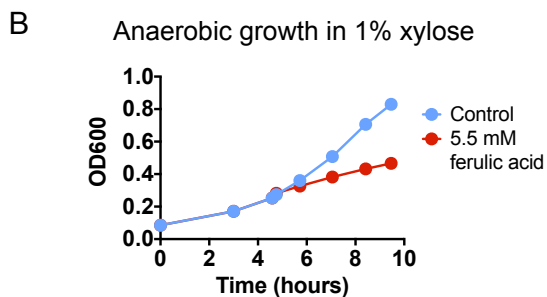
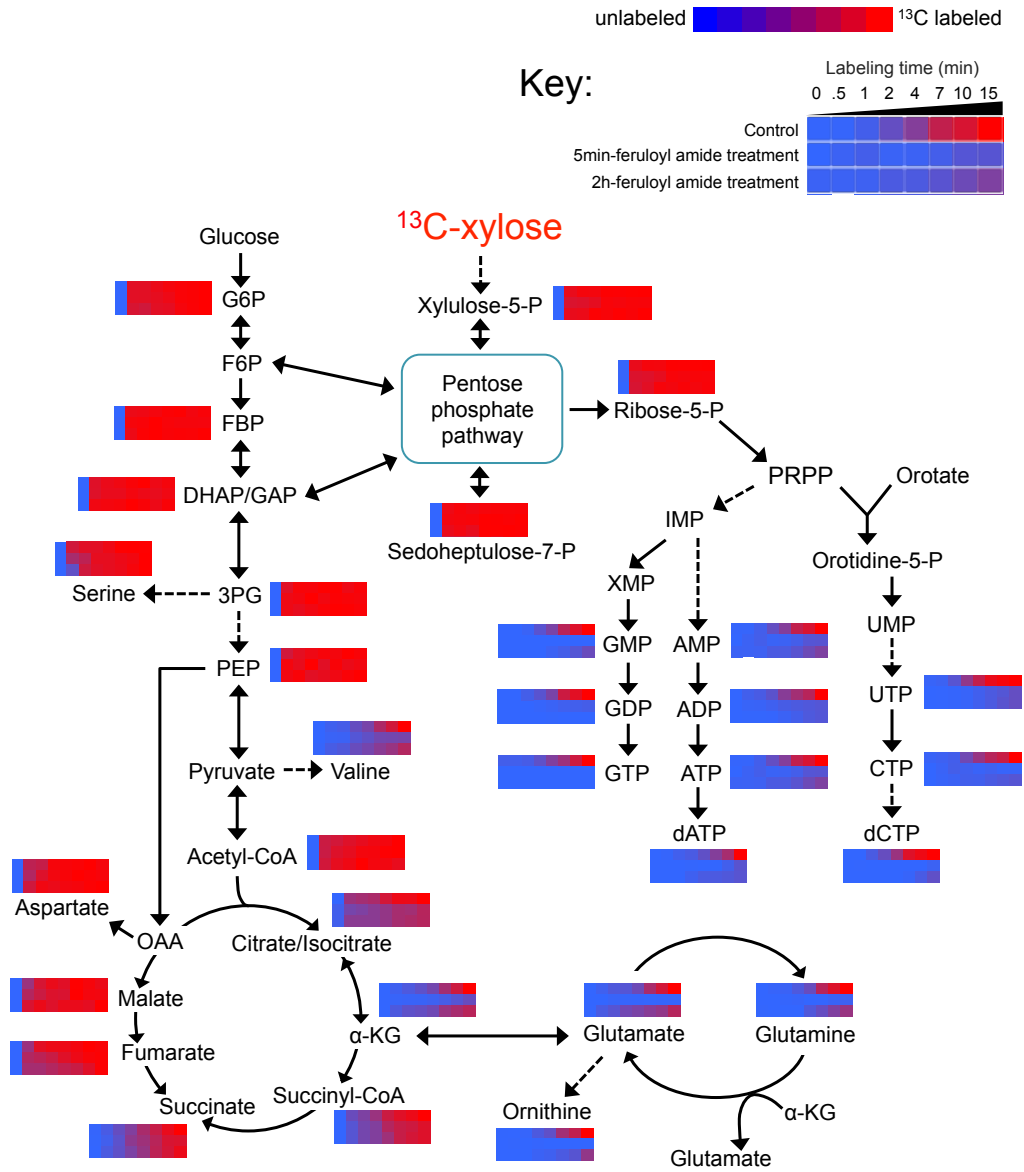


Figure S4

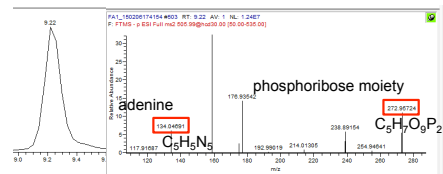
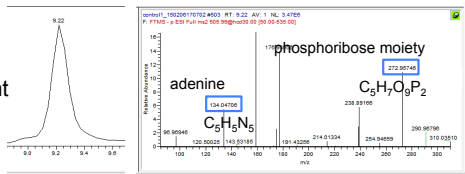


ATP

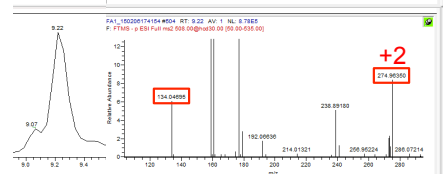
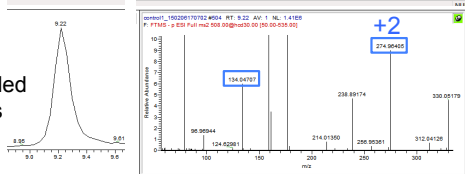
Control

Feruloyl amide

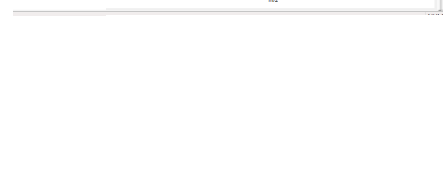
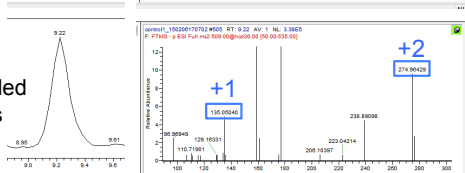
<sup>12</sup>C parent



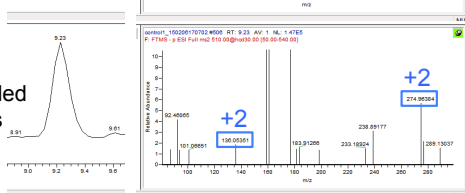
<sup>2</sup><sup>13</sup>C-labeled carbons



<sup>3</sup><sup>13</sup>C-labeled carbons



<sup>4</sup><sup>13</sup>C-labeled carbons

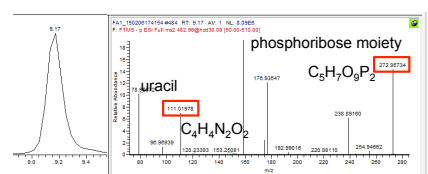
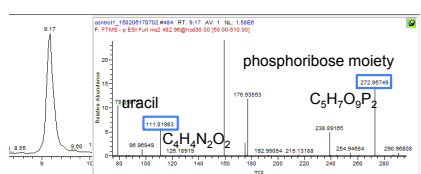


UTP

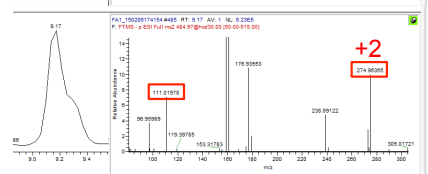
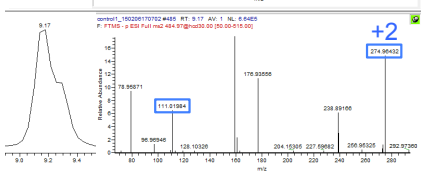
Control

Feruloyl amide

<sup>12</sup>C parent



<sup>2</sup><sup>13</sup>C-labeled carbons



<sup>4</sup><sup>13</sup>C-labeled carbons

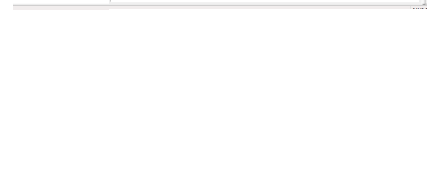
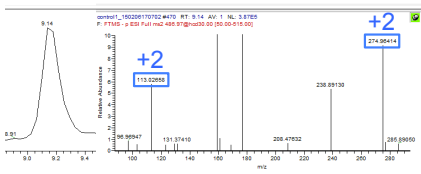
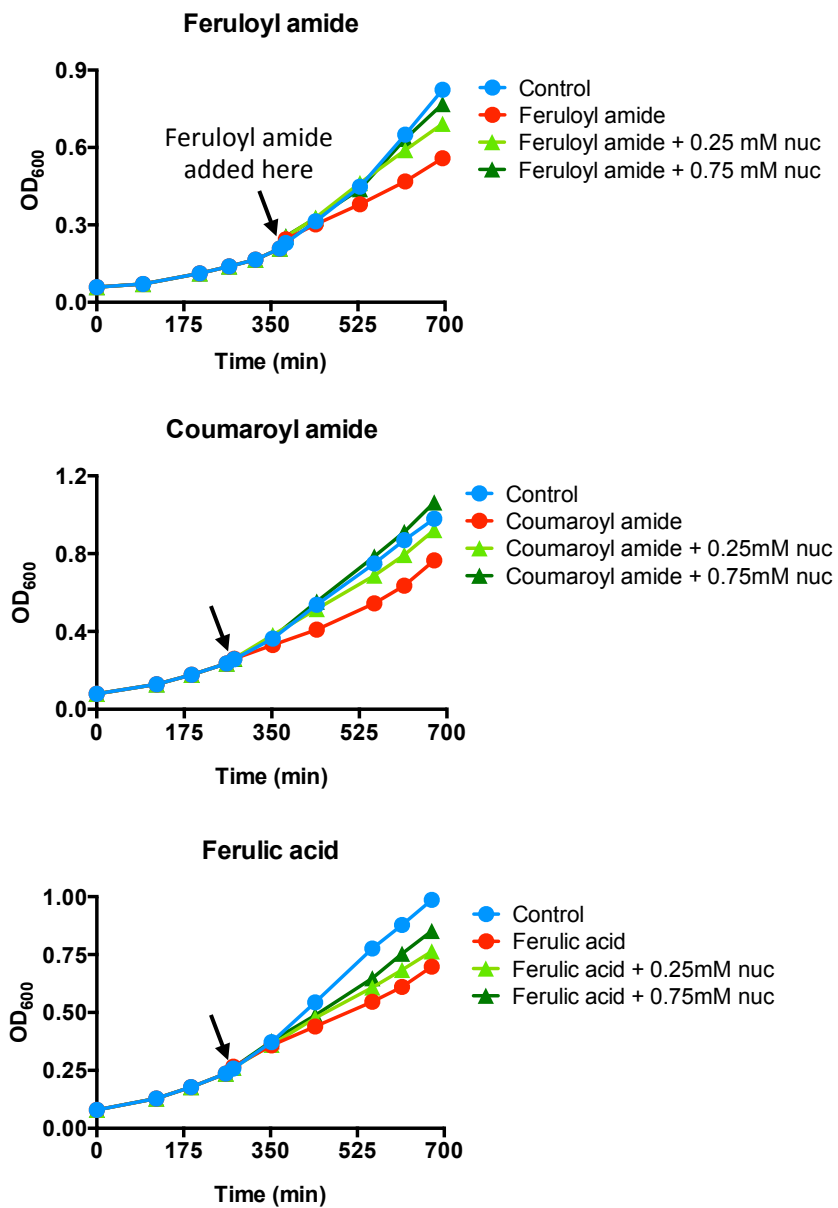
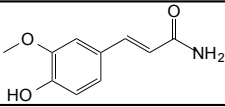
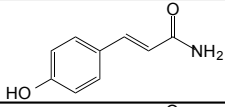
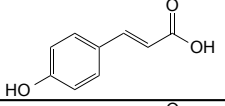
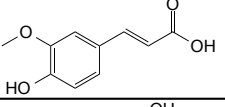
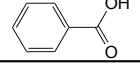
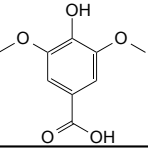
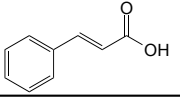
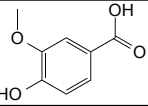
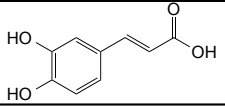
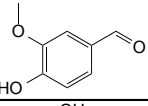
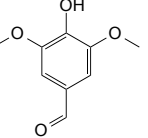
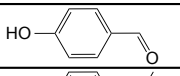
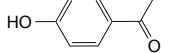




Figure S6



**Supplementary Table S1: Lignocellulose-derived phenolic inhibitors identified in AFEX-pretreated corn stover hydrolysates (Keating, D. H. et al. Front Microbiol 5, 402 (2014))**

Lignotoxins	Structures	Concentrations (mM)
Feruloyl amide		5.5
Coumaroyl amide		5.5
<i>p</i> -Coumaric acid		1.05
Ferulic acid		0.36
Benzoic acid		0.48
Syringic acid		0.08
Cinnamic acid		0.09
Vanillic acid		0.09
Caffeic acid		0.01
Vanillin		0.13
Syringaldehyde		0.16
4-Hydroxybenzaldehyde		0.2
4-Hydroxyacetophenone		0.02

5-Hydroxymethylfurfural (HMF) was not included in this study

**Supplementary Table S2: Target MS/MS parameters used to obtain <sup>13</sup>C labeling patterns of ATP and UTP**

Metabolites	Collision energy	Labeled forms	Mass (m/z)	Fragment mass (m/z) of interest	Molecular formula (neutral)	Names of fragments
ATP	30	non-labeled	505.98846	134.047 272.957	C <sub>5</sub> H <sub>5</sub> N <sub>5</sub> C <sub>5</sub> H <sub>7</sub> O <sub>9</sub> P <sub>2</sub>	Adenine phosphoribosyl moiety
		2 <sup>13</sup> C-labeled carbons	507.99518	134.047 274.964	C <sub>5</sub> H <sub>5</sub> N <sub>5</sub> C <sub>5</sub> H <sub>7</sub> O <sub>9</sub> P <sub>2</sub>	Adenine phosphoribosyl moiety
		3 <sup>13</sup> C-labeled carbons	508.99854	135.050 274.964	C <sub>5</sub> H <sub>5</sub> N <sub>5</sub> C <sub>5</sub> H <sub>7</sub> O <sub>9</sub> P <sub>2</sub>	Adenine phosphoribosyl moiety
		4 <sup>13</sup> C-labeled carbons	510.00189	136.054 274.964	C <sub>5</sub> H <sub>5</sub> N <sub>5</sub> C <sub>5</sub> H <sub>7</sub> O <sub>9</sub> P <sub>2</sub>	Adenine phosphoribosyl moiety
UTP	30	non-labeled	482.96124	111.020 272.957	C <sub>4</sub> H <sub>4</sub> N <sub>2</sub> O <sub>2</sub> C <sub>5</sub> H <sub>7</sub> O <sub>9</sub> P <sub>2</sub>	Uracil phosphoribosyl moiety
		2 <sup>13</sup> C-labeled carbons	484.96796	111.020 272.957	C <sub>4</sub> H <sub>4</sub> N <sub>2</sub> O <sub>2</sub> C <sub>5</sub> H <sub>7</sub> O <sub>9</sub> P <sub>2</sub>	Uracil phosphoribosyl moiety
		4 <sup>13</sup> C-labeled carbons	486.97467	111.020 272.957	C <sub>4</sub> H <sub>4</sub> N <sub>2</sub> O <sub>2</sub> C <sub>5</sub> H <sub>7</sub> O <sub>9</sub> P <sub>2</sub>	Uracil phosphoribosyl moiety

**Other parameters for targeted MS/MS**

Resolution: 35,000

AGC target: 5E5

Isolation width: 1.4 (m/z)

Default charge: 1

Polarity: negative

